



Supplement of

Wintertime subarctic new particle formation from Kola Peninsula sulfur emissions

Mikko Sipilä et al.

Correspondence to: Mikko Sipilä (mikko.sipila@helsinki.fi)

The copyright of individual parts of the supplement might differ from the article licence.

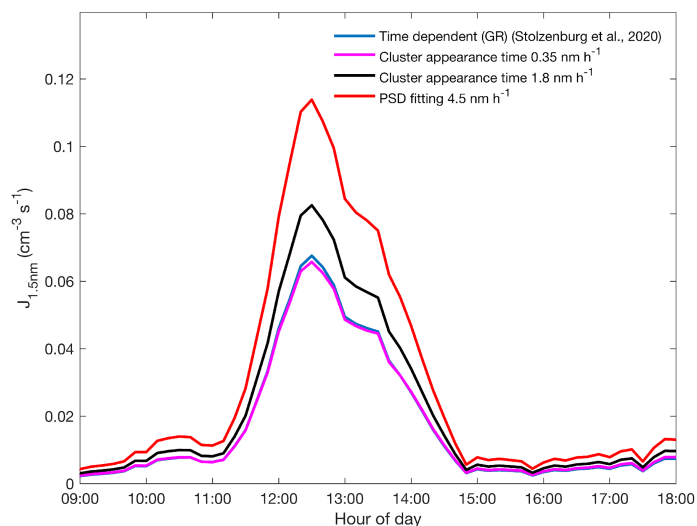


Figure S1. Nucleation rate ($J_{1.5\text{nm}}$) on 29th January 2020 calculated by Eq. 1 using growth rate (GR) calculated from Eq. 3 that assumes irreversible sulphuric acid condensation as sole mechanism of growth (Stolzenburg et al., 2020) (blue line), lower (magenta) and upper (black) limits for GR derived from cluster 50-% appearance time (Lehtipalo et al., 2014) and GR derived from fitting to total particle size distribution (red).

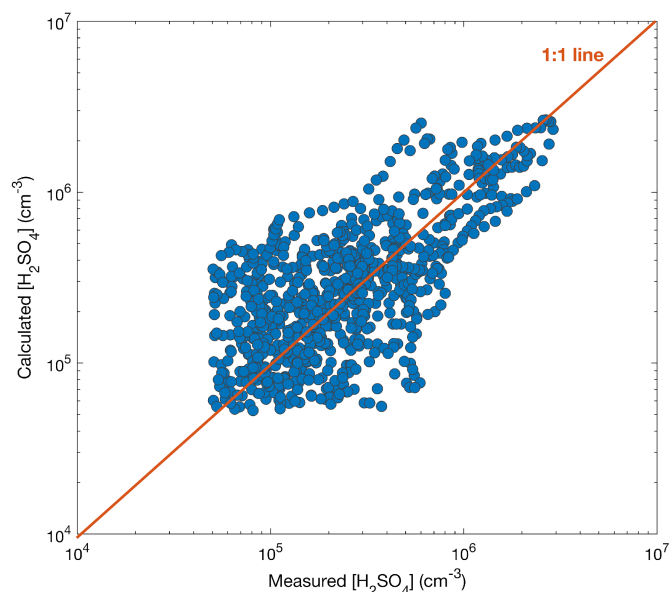


Figure S2. Calculated (Dada et al., 2020) vs. measured sulphuric acid concentration during the whole measurement period when CI-API-TOF data was available.. On average, calculated (Dada et al., 2020) sulphuric acid concentrations agree very well with the measured sulphuric acid concentrations interpolated to same time axis. Difference between the mean concentration is only 8% (Average calculated concentration is 8% larger). This suggests that proxy by Dada et al. (2020) can appropriately describe the winter time sulphuric acid concentrations. Natural fluctuation in data is caused at least by meteorological phenomena such as boundary layer inversion. Here we used a CI-API-TOF approximate lowest detection limit of $5 \cdot 10^4 \text{ cm}^{-3}$ (Jokinen et al., 2012) as a threshold value both for measured and calculated concentration. Data comprises all times when both CI-API-TOF data and data used for proxy calculation were available.

New particle formation and growth during 10th – 12th November 2019

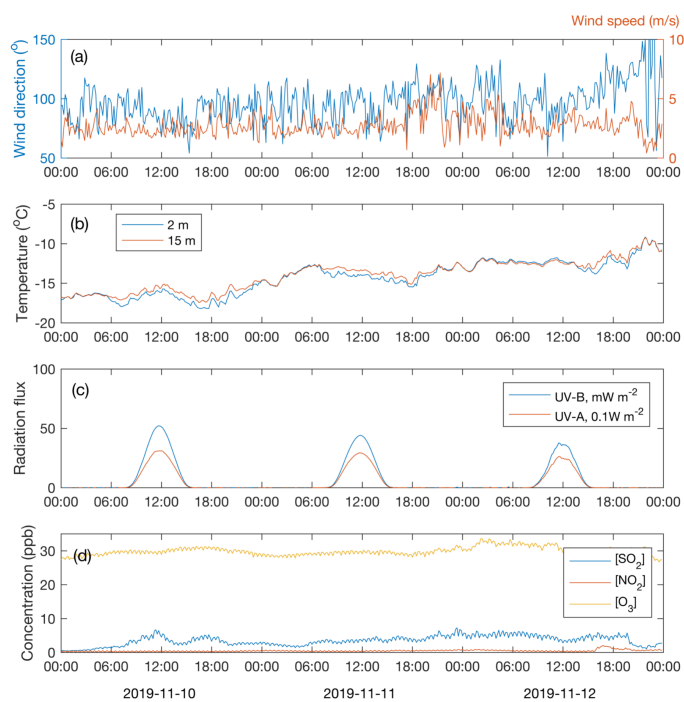


Figure S3. Wind speed and direction at 16 m height (a) , air temperature at two heights (b) , UV-B and UVA radiation (c) and concentrations of SO₂, NO₂, O₃ (d) during 10th-12th November 2019.

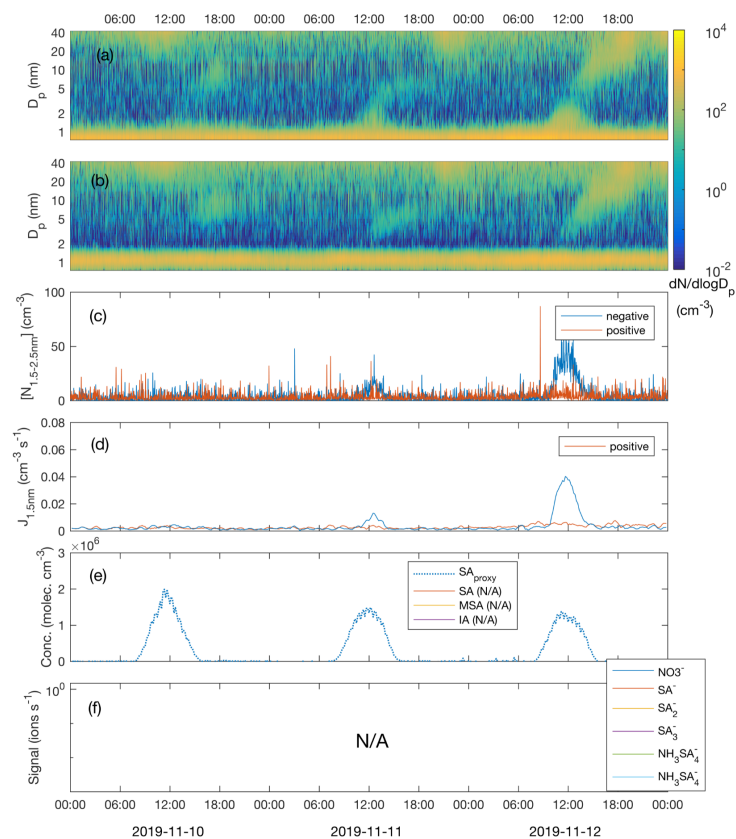


Figure S4. Number size distribution of negative (a) and positive (b) clusters and particles, concentration of freshly nucleated, charged 1.5-2.5 nm clusters (c), formation rate of negative and positive 1.5 nm clusters (d) and sulphuric acid concentration estimated by proxy calculation (e) during 10th – 12th November 2019. CI-API-TOF Mass spectrometer was not operational during the depicted period and thus no measurement data on H₂SO₄, MSA, IA and ion clusters exist.

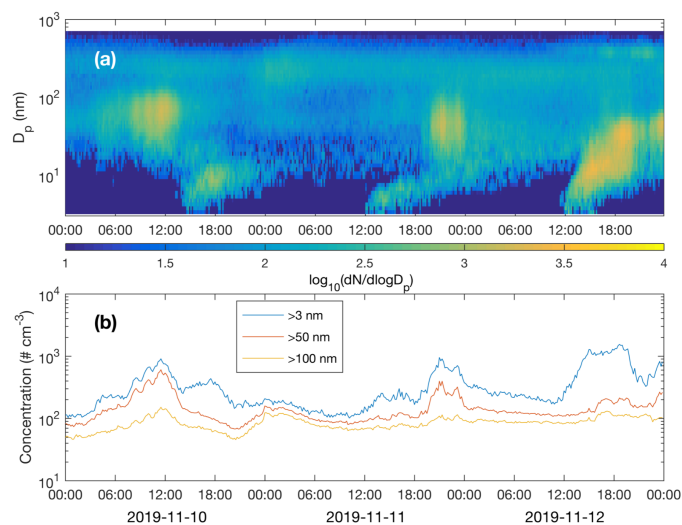


Figure S5. Particle number size distribution (a) and concentrations of particles larger than 3 nm, 50 nm and 100 nm (b) recorded by DMPS during 10th-12th November 2019.

New particle formation and growth 11th March 2020

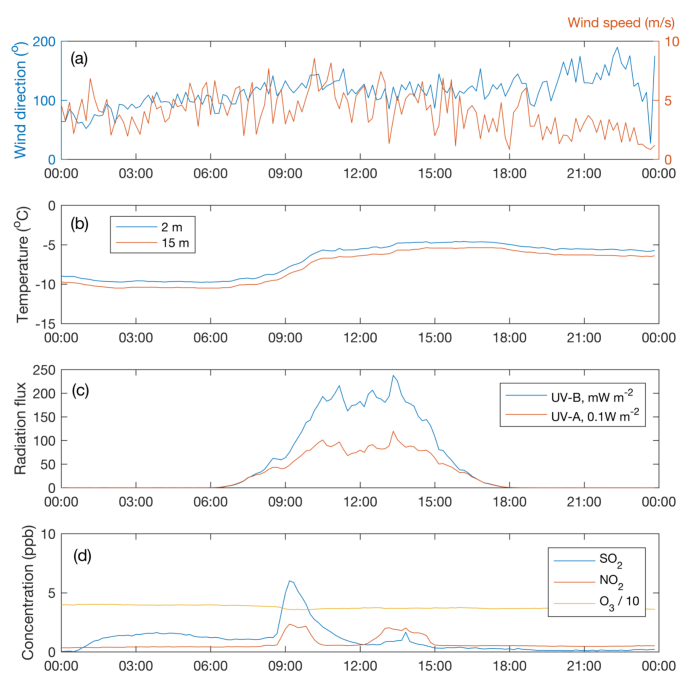


Figure S6. Wind speed and direction at 16 m height (a) , air temperature at two heights (b) , UV-B and UVA radiation (c) and concentrations of SO₂, NO₂, O₃ (d) on 11th March 2020.

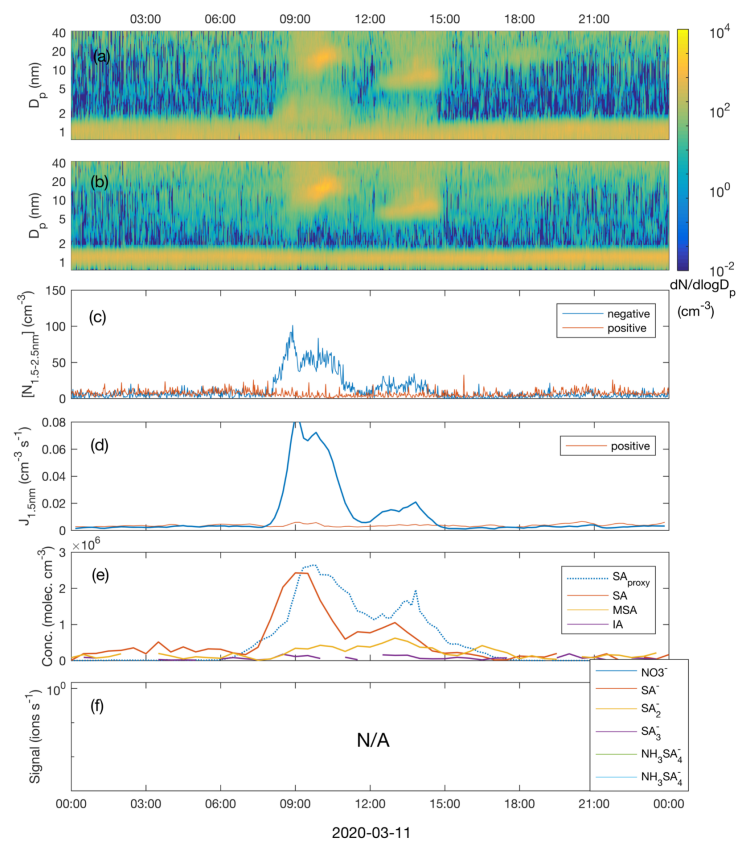


Figure S7. Number size distribution of negative (a) and positive (b) clusters and particles, concentration of freshly nucleated, charged 1.5-2.5 nm clusters (c), formation rate of negative and positive 1.5 nm clusters (d) measured concentrations of sulphuric acid (H_2SO_4), methane sulphonic acid (MSA) and iodic acid (HIO_3) as well as sulphuric acid concentration estimated by proxy calculation (e) on 11th March 2020. Data on ion clusters is not available.

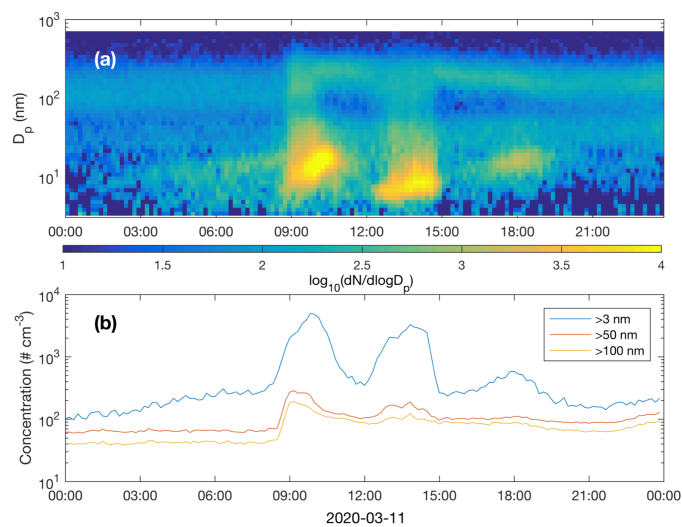


Figure S8. Particle number size distribution (a) and concentrations of particles larger than 3 nm, 50 nm and 100 nm (b) recorded by DMPS 11th March 2020.

New particle formation and growth 3rd December 2019

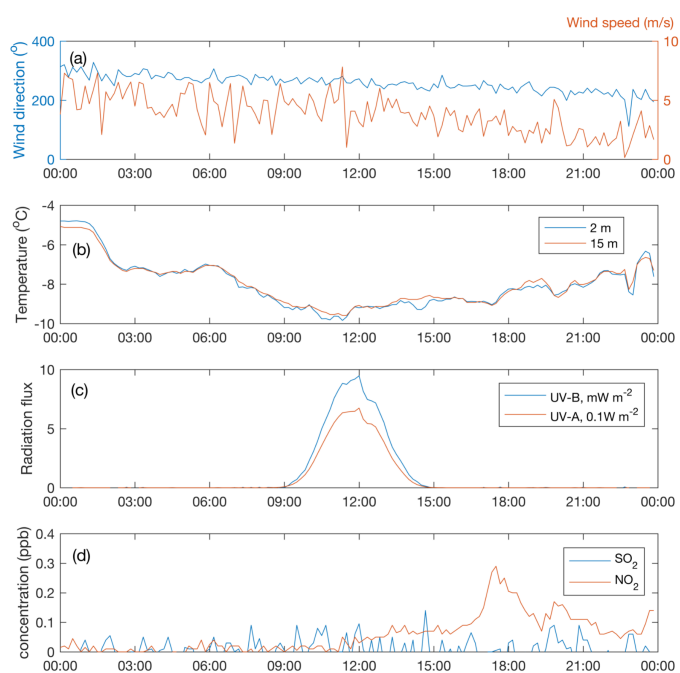


Figure S9. Wind speed and direction at 16 m height (a) , air temperature at two heights (b) , UV-B and UVA radiation (c) and concentrations of SO_2 , NO_2 , O_3 (d) on 3rd December 2019.

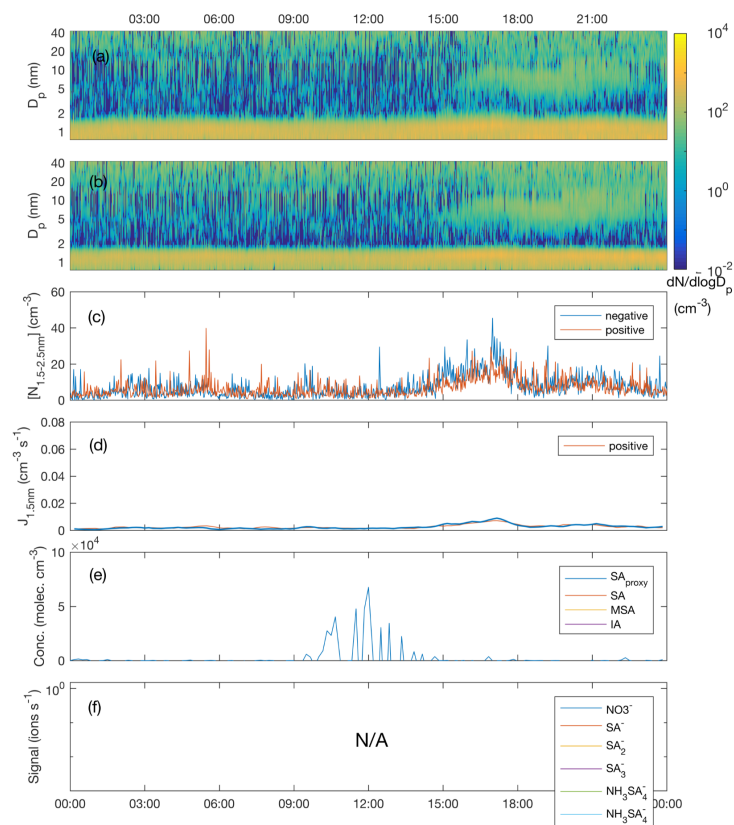


Figure S10. Number size distribution of negative (a) and positive (b) clusters and particles, concentration of freshly nucleated, charged 1.5-2.5 nm clusters (c), formation rate of negative and positive 1.5 nm clusters (d) measured concentrations of sulphuric acid (H_2SO_4), methane sulphonic acid (MSA) and iodic acid (HIO_3) as well as sulphuric acid concentration estimated by proxy calculation (e) on 3rd December 2020. Data on and ion clusters is not available. Nucleation rates are calculated, consistently with the rest of the analyzed days, from the change in concentration $N_{1.5-2.5\text{nm}}$ between 1.5 and 2.5 nm ion clusters. Though the calculation yields non-zero values, from surface plots it is obvious that no growth from cluster sizes to stable particles can be observed. I.e. at least ion-induced nucleation does not occur in situ in proximity of SMEAR. H_2SO_4 , MSA and HIO_3 concentrations were below detection limit of CI-APi-TOF – i.e. no signal was distinguishable from the instrument background. Since $[\text{SO}_2]$ and UVB radiation are close to zero, also calculated H_2SO_4 is negligible and no explanation for formation pathway of observed small particles can be derived from the data. Particles are obviously formed elsewhere and advected to the station or mixed from upper layers of the atmosphere. During the transportation the signs of the particle precursor have been lost.

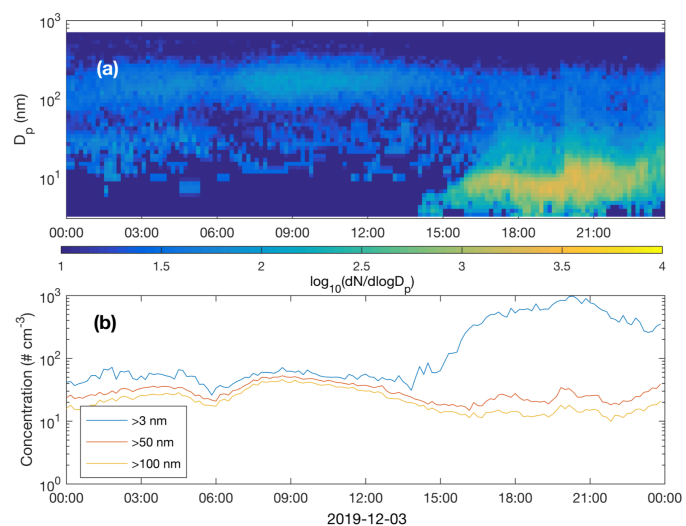


Figure S11. Particle number size distribution (a) and concentrations of particles larger than 3 nm, 50 nm and 100 nm (b) recorded by DMPS 3rd December, 2019.